

# V. ÖRÆFI DISTRICT AND MARKARFLJÓT OUTWASH PLAIN: RATING OF FLOOD HAZARDS

Emmanuel Pagneux \* and Matthew J. Roberts \*

*\* Icelandic Meteorological Office*

## 1. Introduction

In this chapter, a provisional method for the rating of flood hazards is proposed followed by the designation of flood hazard zones in the Markarfljót outwash plain and the Öræfi district, two inhabited regions of Iceland (Figure V-1) that have been subjected during the last millennium to jökulhlaups caused by subglacial eruptions of Katla, Eyjafjallajökull (Gudmundsson *et al.*, 2008; Snorrason *et al.*, 2012), and Öræfajökull volcanoes (Thorarinsson, 1958).

The aim of the study is to provide the national and local authorities with spatial information on flood danger and flood damage potential in the two study areas. The presence of life-threatening debris and the temperature of floodwater are considered, along with depths of flooding and flow velocities; these factors take into account the unique nature of volcanogenic floods. Flood-hazard zones are designated using the results of scenario-based hydraulic simulations performed by Hólm and Kjaran (2005) and Helgadóttir *et al.* (2015) in the Markarfljót outwash plain and in the Öræfi district, respectively. The method presented builds upon selected research on vulnerability of the human environment to floodwaters, including people's vulnerability (e.g. Foster and Cox, 1973; Abt *et al.*, 1989; Keller and Mitsch, 1993; Karvonen *et al.*, 2000; Jonkman and Kelman, 2005; Penning Rowsell *et al.*, 2005; Jonkman and Penning-Rowsell, 2008; Russo *et al.*, 2012) and vulnerability of the built environment (e.g. USBR, 1988; Karvonen *et*

*al.*, 2000; Leone *et al.*, 2010, Valencia *et al.*, 2011).

The scope of the study is limited to an assessment of damage potential within the areas identified at risk of flooding. Characterisation of the likelihood of volcanogenic floods is not addressed. In short, one can describe such floods as hazardous events whose likelihood remains rather uncertain. Indeed, the magnitude and routing of volcanogenic floods depend on several factors, including the nature of ice-volcano interactions and the exact location of eruptions. As a consequence, the long-term probability of a subglacial eruption at a particular location in space and time, and incidentally of the floods it may cause, cannot be specified with confidence. It is estimated for instance that Katla eruptions capable of causing outbursts on the Markarfljót outwash plain have a return period ranging 100 – 1,000 years should they happen in the north-western part (23 km<sup>2</sup>) of the volcano caldera, and 1000–10,000 years should an eruption happen on the western slopes (87 km<sup>2</sup>) of the Mýrdalsjökull ice-cap (Guðmundsson *et al.*, 2005). Concerning Öræfajökull volcano, only two eruptions are known in historical times — the 1362 and 1727 eruptions — that were different in size and location and caused floods in two different glacier catchments (Thorarinsson, 1958; Roberts and Gudmundsson, 2015). For the whole of Iceland, it is estimated that VEI 5 eruptions occur once every 100 – 200 years and VEI 6 eruptions once every 500 – 1000 years (Gudmundsson *et al.*, 2008).

The flood hazard rates proposed here are used for characterising, in the two study areas, exposure of populations to jökulhlaup hazards (Pagneux, 2015a).

The present study is noteworthy for being the first attempt to explore and map flood damage potential in Iceland. Taking into account natural hazards in spatial planning is a legal requirement (Parliament of Iceland, 2010) that is not yet supported, for what concerns riverine floods and glacial

outbursts, by a set of rules describing how hazards and risks should be assessed. The Planning regulation (Ministry for the Environment and Natural Resources, 2013) specifies that it is forbidden to build in areas prone to floods from lakes, rivers, and the sea, irrespective of considerations on a flood return period for which flood hazards and flood risks should be mapped nor on the level of human and material loss beyond which risk is no longer acceptable.

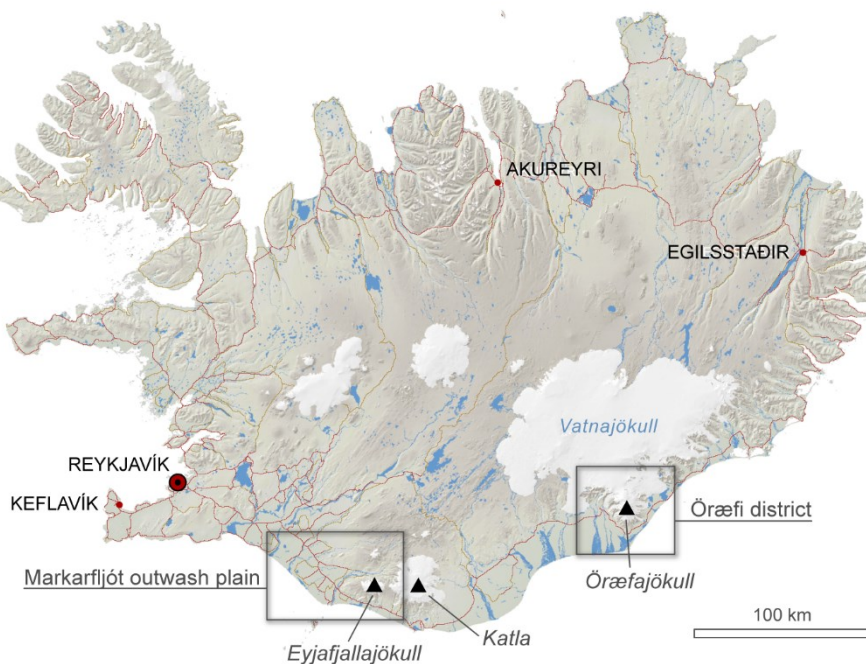


Figure V-1: General location of the Markarfljót outwash plain and Örfæfi district.

### 1.1. Principle of flood hazard rating

Flood hazard “rating” can be thought of as marking off a reference flood into zones, using flood hazard characteristics in excess of which plausible and meaningful adverse consequences such as structural damage or loss of life are likely to occur (i.e. can be predicted at a significant confidence level) (DEFRA, 2006). In this approach, the possibility of events of credible magnitude and plausible outcomes is considered and an assessment of flood damage potential is performed (see §2.3 for examples of flood hazard rating abroad); flood hazard zones are

differentiated primarily on the understanding that fatalities and significant economic damage due a given flood may vary spatially within areas flooded as a consequence of spatial variations in the magnitude of the flood (i.e. flood magnitude considered as a spatial variable), all other things being held equal (i.e. vulnerability purposively considered as a spatial constant). In that respect, rating of flood hazards differs from hazard zoning based on discharge exceedance probabilities (sometimes called “risk zoning”), where risk zones coincide with the spatial extent of flooding events having a known probability of occurrence or an established

return period (de Moel *et al.*, 2009; Figure V-2).

Indeed, the marking-off into zones of a reference flood does not require the flood considered to have a known probability of occurrence. The reference flood may be a

historical event or simply hypothetical. In some cases, the marking-off may refer to an aggregated “worst-case” scenario (e.g. Tinti *et al.*, 2011), as a return period is not known or may appear of little relevance for risk management.

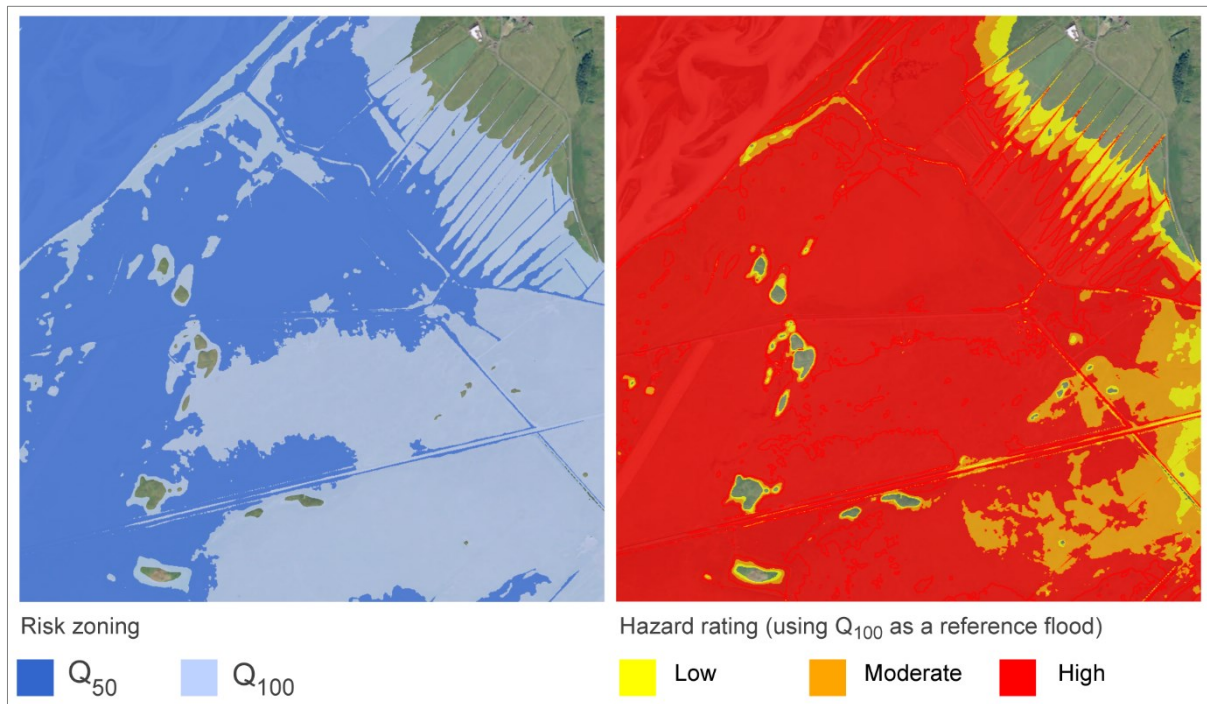


Figure V-2: Fictitious example showing the differences between hazard zoning based on discharge exceedance probabilities — sometimes called “risk zoning”— and hazard rating. In risk zoning (left), spatial extent of flooding events having known return periods, here  $Q_{50}$  (2% chance of occurring in any given year) and  $Q_{100}$  (1% chance) is shown. In hazard rating (right), a reference flood is used, here  $Q_{100}$ , and distinction is made within its spatial extent between levels of danger or damage potential, based on flood hazard characteristics.

## 2. Vulnerability of humans and built environment

The main purpose of hazard rating is not to determine the likelihood of a hazardous event but to map in a sensible manner its potential consequences, including harm to people and damages to structures. It is a prerequisite to an estimation of injury and loss of life in floods, which requires in addition an assessment of the people characteristics (e.g. age, sickness and disabilities) and location within flood areas (Penning Rowsell *et al.*, 2005). It can also serve, coupled to an

inventory of building and structure stocks, in an estimation of monetary losses due to direct damages to exposed physical assets (e.g. Schwarz and Maiwald, 2008; Van Vesten *et al.*, 2014).

Alongside water depths and flow velocities, sediment load and floodwater temperature are flood hazard characteristics that must be considered when tangible damages to buildings and short-term physical effects of floodwaters on humans, inside and outside buildings, are considered.

## 2.1. Damages to buildings

### 2.1.1. Effects of floodwater on buildings

The physical integrity of buildings is threatened by the hydrostatic and hydrodynamic actions of floodwater, scouring, and actions due to the presence of debris (impact loads). Detailed overviews of the physical effects of floods on buildings can be found in Kelman and Spence (2004) and Merz *et al.* (2010).

Hydrostatic actions, which are implied by the presence of water, consist of lateral and vertical pressures against buildings and capillarity rise inside building components. Lateral pressures may lead to the collapse of walls if not counteracted. Buoyancy, which is an uplift force exerted on submerged objects, can result in floating of buildings and may lead, in combination with lateral pressures, to displacement or destruction of buildings. It has been estimated, for example, that unanchored single-storey buildings can begin to float at flood depths of  $> 1.9$  m (Black, 1975). Hydrostatic lateral pressures and capillarity rise can be considered the dominant cause of damage due to riverine floods implying slow rising (Kreibich *et al.*, 2009; Kreibich and Dimitrova, 2010) and long-lasting receding periods.

Hydrodynamic actions, which are due to the motion of water, relate to flow velocities and the formation of waves. Dynamic pressures due to flow velocities and breaking waves are much higher than static pressures due to stagnant waters, and are therefore more likely to cause structural damages to buildings.

Buildings may also be endangered by scouring. Black (1975) and Smith (1989) have estimated that due to severe erosion around foundations, the structural integrity of buildings comes into question at flow velocities higher than 1.5–2 m/s (1.1–2 kPa).

The presence of debris and sediments increases the dynamical forces exerted

against buildings and thus the potential for structural damage, as exemplified by the March 11<sup>th</sup> 2011 tsunami in Great East Japan where concrete blocks removed from coastal defences by floodwater contributed, alongside other debris, to the destruction of thousands of light buildings and overturning of many reinforced concrete structures (Fraser *et al.*, 2013). Drawing a parallel between tsunamis and jökulhlaups is certainly worthwhile in that regard. The weight of boulders and ice blocks that can be mobilised by glacial floods due to volcanic eruptions, geothermal activity, or geological failure can effectively exceed hundreds of tons, as exemplified by recent jökulhlaups in Iceland. The 15 April jökulhlaup (peak discharge 10,000–15,000 m<sup>3</sup>/s) caused by the Eyjafjallajökull 2010 eruption left thousands of clasts of glacier ice along the flood route, sizing each up to 5 t at nearly 5 km from the glacier margin (Figure V-3). During the 2010 Eyjafjallajökull eruption, an ice slurry flowing across the surface of Gígjökull and descending via a bedrock col adjacent to the main flood corridor managed to displace a 4,000 t boulder on a steep slope (Roberts *et al.*, 2011). Similarly, the 1999 jökulhlaup from Sólheimajökull (peak discharge ~4400 m<sup>3</sup>/s) mobilised boulders up to 11 m in diameter (Russell *et al.*, 2010). During the 1996 glacial outburst on the Skeiðarársandur outwash plain (peak discharge 55,000 m<sup>3</sup>/s), ice blocks 10–20 m in diameter were also filmed rolling down by the National road, 5–7 km away from the glacier margin (Figure V-4).

### 2.1.2. Damage functions and thresholds

Flood characteristics such as flood depths, flow velocities, impact pressures, and debris heights can be used, separately or in combination, in functions aimed at the prediction of damage to buildings (also known as vulnerability curves or fragility curves).

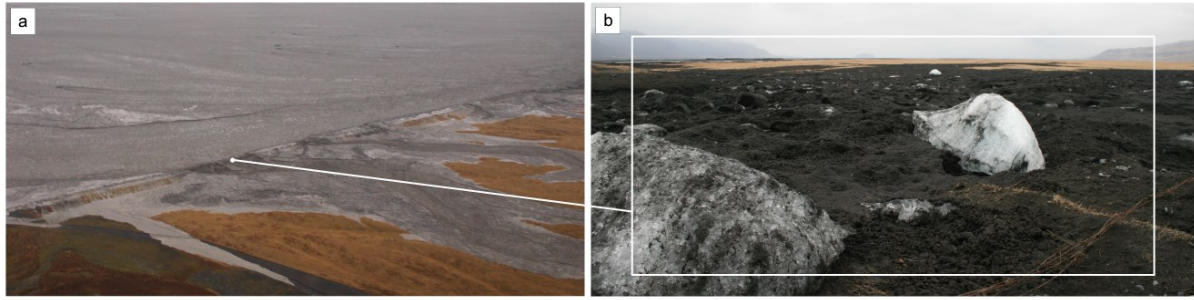


Figure V-3: (a) April 15 2010 jökulhlaup caused by eruption of Eyjafjallajökull volcano. Minutes after the flood begins, floodwater rapidly overtops a first levee, 5 km away from the glacier margin, which shows early signs of failure at several locations due to excessive flow velocities and impact of ice blocks (Credit: Matthew J. Roberts). In the end, 300 metres of levees were swept away. (b) Downstream view taken on April 30 2010 from the levee (failure location), showing hundreds of clasts of glacier ice, 1–5 t in size in a matrix of volcanic mud (Credit: Emmanuel Pagneux).



Figure V-4: Remnants of stranded ice blocks transported by floodwater during the November 1996 glacial outburst on the Skeiðarársandur outwash plain (peak discharge 55,000 m<sup>3</sup>/s). Note the 1.70 m tall adult standing between the blocks. Credit: Oddur Sigurðsson, January 4 1997.

Depths of flooding and flow velocities can be combined for instance in a qualitative manner, using a matrix (e.g. MATE/METL, 2002), or as a quantitative aggregate, referred in the literature to as depth-velocity product, labelled  $dv$  or  $hv$  and expressed in m<sup>2</sup>/s (e.g. Clausen and Clark, 1990; Karvonen *et al.*, 2000). Impact pressures (Wilhelm, 1998; Barbolini *et al.*, 2004) or debris heights (Fuchs *et al.*, 2007; Akbas *et al.*, 2009; Luna *et al.*, 2011) can be used alternatively in the definition of damage functions for gravity driven phenomena, such as hyperconcentrated flows, debris-flows, and avalanches.

As the actual level of damage is not only a consequence of flood characteristics but also of design, damage functions need to consider flood characteristics in relation to classes or types of buildings. A distinction is made in the literature between wooden and concrete structures (Karvonen *et al.*, 2000; Dutta *et al.*, 2003), anchored and unanchored structures (Karvonen *et al.*, 2000), and single storey and multiple-storey buildings (Black, 1975; Smith, 1991; Leone *et al.*, 2010) to name a few. An example of detailed classifications recently proposed is given in Schwarz and Maiwald (2008) who, in the aftermath of floods from the Elbe river that struck

Germany in 2002, 2005, and 2006, made an inventory of the building stock using the following six categories: clay, prefabricated, framework, masonry, reinforced concrete, and flood-proof.

Particular thresholds deserve attention when habitation buildings are considered, as they may mark, in the absence of better information, the lower boundary of zones of “total devastation”:

- Total destruction of brick and masonry buildings can be expected at depth-velocity products  $dv > 7 \text{ m}^2/\text{s}$  (Clausen and Clark, 1990; Karvonen *et al.*, 2000; Table V-1).

Valencia *et al.* (2011) estimated, after transposition to the European built environ-

ment of the empirical findings from Leone *et al.* (2010) on damages to buildings due to the 2004 tsunami in Banda-Aceh (Indonesia), that structural damage to reinforced concrete buildings that require demolition in the recovery phase should be expected where depths of flooding  $> 6 \text{ m}$  (Table V-2).

- When gravitational flows are considered, total destruction of single to three-storey brick masonry and concrete structures can be expected at debris height ranging 2.5 m (Akbas *et al.*, 2009) to 3.6 metres (Luna *et al.*, 2011).
- Structures impacted by flows can be considered beyond repair in case of impact pressures  $> 34 \text{ kPa}$  (Wilhelm, 1998; Barbolini, 2004).

*Table V-1: Identified flow conditions causing partial or total structural damage of Finnish houses in the EU-project RESCDAM (After Karvonen *et al.*, 2000). Flow velocities alone and/or the product of flow velocities and water depths, referred in the literature as depth-velocity product ( $dv$ ) are used.*

House type	Partial damage	Total damage
Wood-framed		
Unanchored	$dv \geq 2 \text{ m}^2/\text{s}$	$dv \geq 3 \text{ m}^2/\text{s}$
Anchored	$dv \geq 3 \text{ m}^2/\text{s}$	$dv \geq 7 \text{ m}^2/\text{s}$
Masonry, concrete & brick	$v \geq 2 \text{ m/s}$ and $3 > dv > 7 \text{ m}^2/\text{s}$	$v \geq 2 \text{ m/s}$ and $dv \geq 7 \text{ m}^2/\text{s}$

*Table V-2: Depth-damage matrix adopted in the SCHEMA project (After Valencia *et al.*, 2011).*

Building classes	I. Light	II. Masonry, and not reinforced concrete	III. Reinforced concrete	
Height and storeys	0 to 1 level, rarely 2	1 to 3 levels	0 to 3 levels	
Damage levels	Actions	Depths of flooding		
D1, Light damage	Immediate occupancy / repairable	$< 1.8$	$< 2$	$< 3$
D2, important damage	Evacuation / repairable	$1.8 < d < 2.2$	$2 < d < 4.5$	$3 < d < 6$
D3, Heavy damage	Evacuation / demolition required	$2.2 < d < 2.6$	$3 < d < 6.5$	$6 < d < 9.5$
D4, Partial collapse	Evacuation / demolition required	$2.6 < d < 3.8$	$4 < d < 9$	$9.5 < d < 12.5$
D5, Total collapse		$> 3.8$	$5 < d < 9$	$> 12.5$

## 2.2. Human safety

Since the early 1970s, the short-term physical effects of floods on human life have been mainly analysed from the angle of human instability in floodwaters. Two hydrodynamic mechanisms, causing instability at depths of flooding not exceeding a person's height, have been identified (Jonkman and Penning-Rowse, 2008):

- Toppling (moment instability), which relates to the depth-velocity product  $dv$ ;
- Sliding (frictional instability), which relates to the  $dv^2$  product.

Early experiments on pedestrians' safety suggest a critical depth-velocity product  $dv_c$  ranging 0.16–0.52  $m^2/s$  for children aged 9–13 years (Foster and Cox, 1973). Keller and Mitsch (1993) estimated  $dv_c$  ranging 0.21–0.32  $m^2/s$  for a 5-year old child 1.11 m tall and weighing 19 kg, i.e. a critical velocity of 0.5 m/s for a 0.6 m depth of flooding. Abt *et al.* (1989) suggest a  $dv_c$  ranging 0.71–2.13  $m^2/s$  for adults. Experiments realised during the RESCDAM project (Karvonen *et al.*, 2000) suggest a lower critical  $dv_c$ , ranging

0.64–1.26  $m^2/s$ . A recent study from Jonkman and Penning-Rowse (2008) indicates that human instability due to toppling is dominant at depths  $> 0.8$  metre and corresponds to a constant  $dv_c = 1.32 m^2/s$  for an individual 1.75 m tall and weighing 75 kg (Figure V-5). At depths of flooding  $< 0.8$  metre, sliding becomes the dominating phenomenon and is likely the mechanism prevailing in urban floods where shallow waters are associated with excessive velocities. Russo *et al.* (2012) propose a critical velocity  $v = 1.88 m/s$  at flow depths 15–20 cm.

As for pedestrians, safety of car users and passengers has been analysed until now under the prism of thresholds in flow velocities and water depths. An early study on passengers' safety in the case of a dam break published by the US Bureau of Reclamation (1988) suggests that automobilists of "almost any size" are in danger in stagnant waters when depth of flooding is in excess of 1 m, the threshold in water depth being decreased to 0.7 m at flow velocity  $\sim 2 m/s$ . More recently, critical depth-velocity products  $dv_c$  0.25 for children and 0.7 for adults have been proposed (Reiter, 2000).

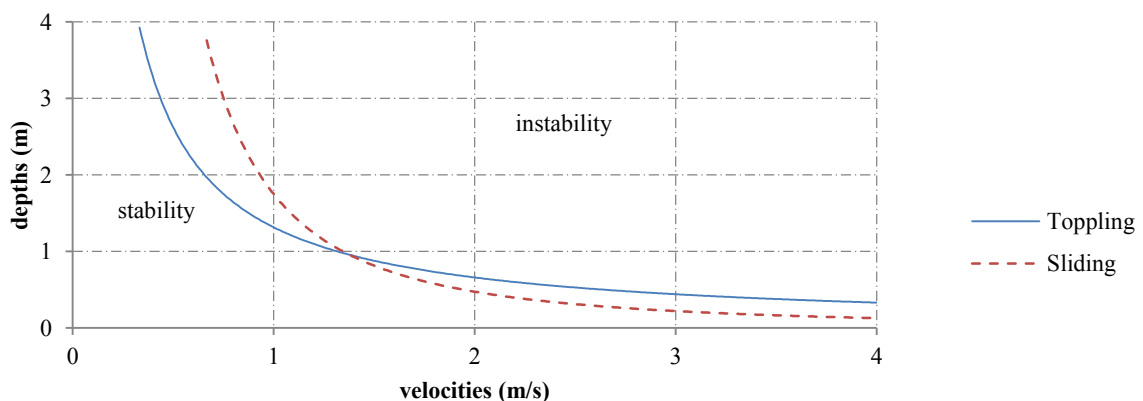


Figure V-5: Theoretical boundary between stability and instability in flood waters for an individual  $m = 75 kg$  and  $L = 1.75 m$ . Instability due to toppling is reached at depth-velocity product  $dv$  1.3  $m^2/s$ . Modified from Jonkman and Penning-Rowse (2008).

The depth-velocity products  $dv$  and  $dv^2$  are only an approximation of the ability of individuals to remain in control in floodwater

in real conditions. Stress, poor lighting or darkness, disabilities, water temperature or injuries due in particular to transported

debris, all contribute to a significant attenuation of stability in floodwater and therefore increase the risk of drowning, which has been identified as the dominant mode of death when riverine floods and flash floods are considered (French *et al.*, 1983). It should be observed, in particular, that the question of instability in floodwater is of a limited relevance when hyper-concentrated flows and debris flows (sediment load > 60%) are considered. In such situations, injuries and short-term fatalities may relate directly to debris (see §2.1.1) and excessive sediment loads. Most of the fatalities due to lahars triggered by the 1985 eruption of Nevado Del Ruiz Volcano (~25,000 deaths) concerned people that became trapped in the mud and debris and were eventually buried by the flows of sediments (Voight, 1990; Mileti *et al.*, 1991). The Nevado Del Ruiz 1985 event exemplifies the potency of floods triggered by volcanic eruptions, emphasising the necessity of identifying areas that are at risk of volcanogenic floods.

Finally, jökulhlaups and lahar pulses generated by a volcanic eruption can be alternatively ice-cold or burning hot. For instance, a temperature of 92 °C was reported at a one-foot depth in a lahar deposit due to the 1919 eruption of Kelut volcano (East Java, Indonesia), a few days after it had formed (Kemmerling, 1921). The risk of severe burning should therefore be kept in mind, as well as the risk of drowning due to accidental hypothermia (Lloyd, 1996) and numbness-related loss of stability.

### 2.3. Rating methods

The choice of input parameters and thresholds is quite variable between countries and may look, for this reason, somewhat arbitrary. In reality, the methods in the selection and use of the parameters depend on their availability and on the adverse consequences considered: human safety, damages

to building, emergency response, compensation schemes, etc.

In northern America, zoning is most often performed using the 100-year flood as a reference. A distinction is made there between the floodway, which includes the main channel and the adjacent overbank areas of greatest water depths and flow velocities, and the flood fringe, where depths and velocities are lower (Environment Canada, 1993; NARA, 2009). A one-foot depth is usually retained to differentiate between the flood way and the fringe. In France and in Austria, flood depths and flow velocities corresponding to a computed 100-year flood are combined and itemised into low, moderate, and high danger classes (MATE/METL, 1999; EXIMAP, 2007). In the UK, rating of hazards due to riverine floods relies on a 4-point classification of the 100-year and 1000-year floods (Table V-3), where harm potential of floating debris recruited is added to the depth-velocity product (DEFRA, 2006; DEFRA, 2008).

In the absence of hydraulic modelling, flow speeds may be deduced from the course of floating objects but at specific locations only. In reality, depths of flooding or debris heights are most often the only empirical data available and therefore the main characteristic considered when it comes to mark off a flooding event into danger zones (MATE/METL, 1999) and develop damage functions based on empirical evidence (e.g. Leone *et al.*, 2010; Valencia *et al.*, 2011).

## 3. Methodology

Thresholds in computed depths of flooding and flow velocities on the one hand, presence of life-threatening debris and temperature of floodwaters on the other, were used to perform a danger-oriented, semi-quantitative rating of flood hazard.

Table V-3: Safety-to-person classification of flood hazard adopted in the UK (DEFRA, 2006; DEFRA, 2008).

<b>Rating formula</b>	<b>Hazard rate = <math>d(v + n) + DF</math></b> <b><math>d</math> = depth of flooding (m);</b> <b><math>v</math> = velocity of floodwaters (m/s);</b> <b>DF = debris factor (0, 0.5, 1 depending on probability that debris will lead to a hazard)</b> <b><math>n</math> = a constant of 0.5</b>	
<b>Flood hazard rates</b>	<b>Colour scheme</b>	<b>Hazard to People Classification</b>
Less than 0.75	-	Very low hazard – Caution
0.75 to 1.25	Yellow	Danger for some – includes children, the elderly and the infirm
1.25 to 2.0	Orange	Danger for most – includes the general public
More than 2.0	Red	Danger for all – includes the emergency services

### 3.1. Rules of rating

A distinction is made between four flood hazard rates: low (1), moderate (2), high (3) and extreme (4), described below and summarized in Table V-5. An additional category (-99) is used when flood hazard cannot be rated.

Computed depth-velocity products  $dv$  should be used when depths of flooding and flow velocities are known. Water depths  $d$  can be used alone when information about flow velocities  $v$  is missing.

The peculiar rheologies of volcanogenic floods is addressed by taking into account the presence of life-threatening debris and sediments, decided on expert judgement: index  $l$  is set to 1 when debris are estimated life-threatening, otherwise  $l$  is set to 0;  $l$  should be set to NULL if not determined. Judging of the presence of life-threatening debris is particularly recommended when information on flow velocities and depths of flooding is missing.

The risk of severe injuries and fatalities due to temperature of floodwater, both stagnant and moving, can be taken into account when deemed relevant using expert judgement: index  $t$  is set to 1 when water temperature implies severe injuries or fatalities; otherwise  $t$  is set to 0;  $t$  should be set to NULL if not determined.

The time available for evacuating areas at risk of flooding (addressed in Pagneux, 2015b) is not formally taken into account in the methodology.

#### 3.1.1. Level of hazard undetermined

Flood hazard should be rated as “undetermined” (-99) when depths of flooding  $d$  and flow velocities  $v$  are not known or cannot be inferred and the impact of debris and sediment load  $l$  and of water temperature  $t$  remains unevaluated; Value of  $d$ ,  $v$ ,  $l$ , and  $t$  is then set to NULL.

#### 3.1.2. Low hazard

Hazard should be rated as *low* if  $dv < 0.25 \text{ m}^2/\text{s}$ . When flow velocities  $v$  are not known,  $dv$  is replaced by  $d < 0.5 \text{ m}$  (it is assumed that  $v < 0.5 \text{ m/s}$  when  $d < 0.5 \text{ m}$ ).

Injuries or fatalities are unlikely. Damages are mostly limited to furniture inside buildings.

#### 3.1.3. Moderate hazard

Hazard should be rated as *moderate* if sediment load index  $l = 0$  and floodwater temperature index  $t = 0$  and  $dv$  is between  $0.25\text{--}3 \text{ m}^2/\text{s}$ . When flow velocities are not known,  $dv$  can be replaced by  $d$  ranging  $0.5\text{--}1 \text{ m}$ .

Danger is for some, including children, the elderly and the infirm, inside and outside buildings. Damages to buildings are expected but the structural integrity of buildings remains preserved.

### 3.1.4. High hazard

Hazard should be rated as *high* if  $dv > 1.3 \text{ m}^2/\text{s}$  or sediment load index  $l=1$  or floodwater temperature index  $t=1$ . When flow velocities are not known,  $dv$  can be replaced by  $d > 1 \text{ m}$ .

All lives are in jeopardy, outside and inside habitation buildings. The risk of drowning is significant as the wading limit for a normalised adult is reached; severe injuries or fatalities due to debris load and temperature of floodwaters may be expected.

Partial or total collapse of light buildings is expected due to scouring, buoyancy, and lateral pressures exerted against walls.

### 3.1.5. Extreme hazard

Hazard can be rated as *extreme* when  $dv \geq 7 \text{ m}^2/\text{s}$ , irrespective of considerations on debris and temperature of floodwaters. When flow velocities are not known,  $dv$  can be replaced by  $d > 6 \text{ m}$ .

Total destruction of non-reinforced buildings is expected. Structural damages to reinforced concrete dwellings are expected to a degree that would require demolition in the recovery phase.

## 3.2. Visualisation

Hazard rates are displayed as a layer of surficial tints showing on top of a basemap. Each rate is represented by a unique colour code, ranging from yellow to brown (Table V-5). Grey colour is used when the level of hazard is not determined.

## 4. Flood models and geomorphic evidence

### 4.1. Markarfljót outwash plain

Simulation of a glacial outburst flood originating from Entujökull glacier performed by Hólm and Kjaran (2005) was used for the rating of flood hazard. A maximum discharge of  $300,000 \text{ m}^3/\text{s}$  estimated by the National Road, and an average Manning roughness coefficient  $n = 0.1 \text{ s/m}^{1/3}$  were used in the simulation, the output readily available being the maximum depths of flooding. It should be noted that the simulation made no account for sediment erosion and deposition. Results of the simulation indicate an inundation area of  $\sim 810 \text{ km}^2$ , extending all the way from the glacier margin west to the Þjórsá river, 75 km away (Figure V-6).

The DEM used in the numerical simulation by Hólm and Kjaran (2005) was derived from elevation contours ranging 0.5–1 metre below 50 metres ASL, 2-metres contours between 50 and 70 metres ASL, 2.5-metres contours between 70 and 100 metres above ASL, and contours ranging 5–10 metres above 100 metres ASL. As changes in altitude, and not slope variations, were used therein to decide of the contour intervals, one cannot expect the results of the simulation to be particularly reliable in nearly-flat areas. Moreover, the flood area identified in the simulation is contiguous, south from Eyjafjallajökull volcano, to the spatial boundary of the hydraulic model. Considering the rheological settings of the simulation and the depths of flooding found at the boundary of the model, it is likely that floodwater would have propagated further to the east had a larger topographic envelope been used in the simulation. Based on an analysis of elevation contours beyond the model boundaries, it seems reasonable to make a  $33 \text{ km}^2$  addition to the flood area, extending east to the Holtsós coastal lagoon (Figure V-6).

Table V-4: Provisional flood hazard rates proposed. Each hazard rate is verified if value of *d*, *dv*, *l*, or *t* is true. Depth-velocity product has precedence on other flood hazard characteristics.

Hazard rate	Quantitative thresholds		Qualitative thresholds		Damages to buildings	Casualties
	<i>dv</i> (m <sup>2</sup> /s) *	<i>d</i> (m) **	<i>l</i> ***	<i>t</i> ****		
<i>Low</i>	< 0.25	< 0.5	n.a.	n.a.	Mostly limited to furniture inside buildings	Injuries or fatalities are unlikely
<i>Moderate</i>	0.25–1.3	0.5–1	n.a.	n.a.	Damages to buildings expected but structural integrity of buildings preserved	Danger for some (including children, the elderly and the infirm) inside and outside buildings
<i>High</i>	> 1.3	> 1	1	1	Partial or total collapse of light buildings expected	All lives in jeopardy, outside and inside habitation buildings
<i>Extreme</i>	≥ 7	> 6	n.a.	n.a.	Total destruction of non-reinforced buildings expected. Structural damages to reinforced concrete dwellings expected to a degree that would require demolition in the recovery phase	All lives in jeopardy, outside and inside habitation buildings

\* Flood depth - flow velocity product    \*\* Flood depth    \*\*\* Debris and sediment load index    \*\*\*\* Water temperature index

Table V-5: Flood hazard rates and corresponding colour codes. Screen colours values (RGB) are given in brackets.

Hazard rate	Code	Colour
Undetermined	-99	Grey (190, 190, 190)
Low	1	Yellow (255, 255, 0)
Moderate	2	Orange (255, 165, 0)
High	3	Red (255, 0, 0)
Extreme	4	Brown (128, 0, 0)

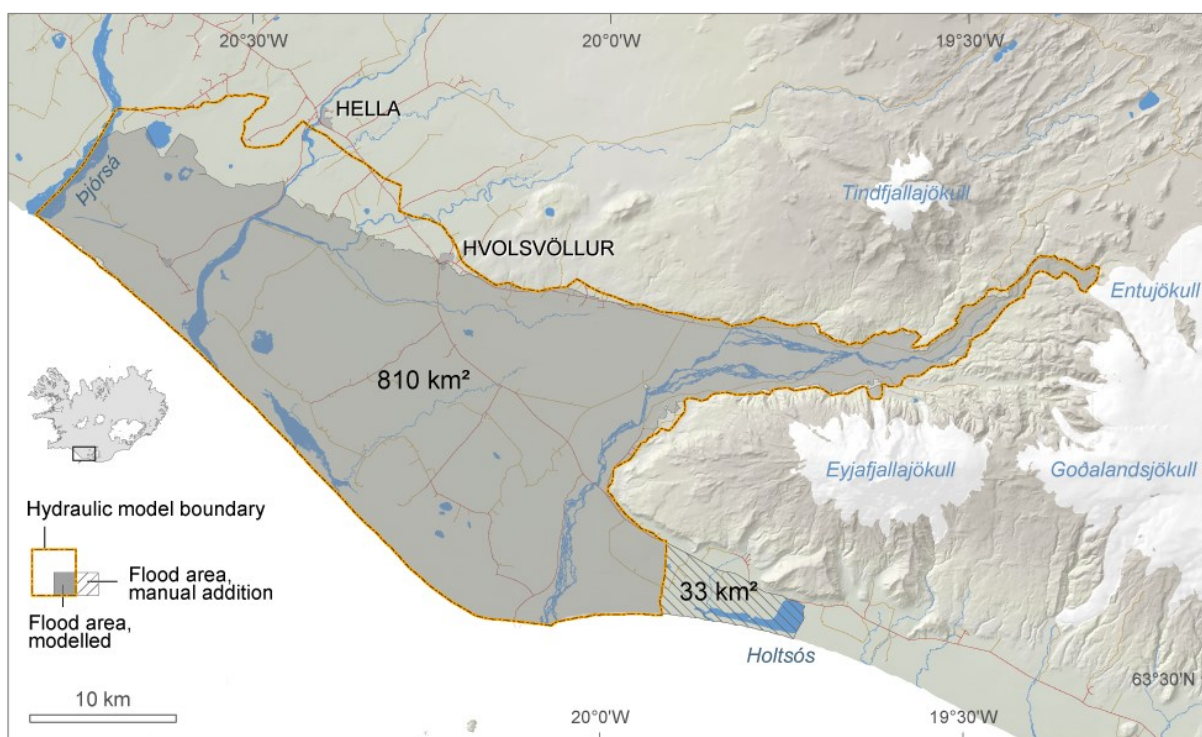


Figure V-6: Area identified at risk of flooding (greyish area) in the Markarfljót outwash plain due to volcanic activity under the Mýrdalsjökull ice-cap (Hólm and Kjaran, 2005). A maximum discharge of  $300,000 \text{ m}^3/\text{s}$  estimated by the National Road and an average Manning roughness coefficient  $n=0.1 \text{ s/m}^{1/3}$  were used as inputs in the simulation. A manual extension of the flood area (striped pattern) beyond the boundaries of the hydraulic model is added, based on an analysis of elevations contours.

## 4.2. Öräfi district

For the Öräfi region, information on depths of flooding and flow velocities was extracted from numerical simulations performed by Helgadóttir *et al.* (2015) (Figure V-7). The simulations were performed within the spatial limits, here referred to as hydraulic model boundary, of a 5 m cell-size Digital Elevation Model (DEM) that covers the Öräfajökull ice-cap and its non-glaciated surrounds. The DEM originates from an airborne LiDAR survey performed during the summers of

2011 and 2012. The vertical accuracy of the LiDAR measurements and the average density of the point cloud are estimated  $< 0.5 \text{ m}$  and  $\sim 0.33 \text{ point/m}^2$ , respectively (Jóhannesson *et al.*, 2011; Jóhannesson *et al.*, 2013).

The simulations build upon melting scenarios in which melting of ice and snow is caused alternatively by (i) eruptions in the caldera and on the flanks of Öräfajökull ice-capped stratovolcano, and the (ii) formation of pyroclastic density currents (Gudmundsson *et al.*, 2015). The floods were simulated as

instant release waves of water flowing at the surface of the glacier, using predefinitions of peak discharge at the glacier margins ranging 10,000 - 100,000 m<sup>3</sup>/s and average Manning roughness coefficients  $n$  ranging 0.05–0.15 s/m<sup>1/3</sup>. It should be noted that the simulations made no account for sediment erosion and deposition. The results of the individual simulations were combined into one aggregated hazard scenario describing the maximum depths of flooding and maximum flow velocities that can be expected at every location within the 237 km<sup>2</sup> of land identified at risk of flooding within the spatial limits of the hydraulic model.

Helgadóttir *et al.* (2015) completed the cartography of the flood area beyond the boundaries of the hydraulic model by analysing sub-metre resolution aerial imagery taken by *Loftmyndir ehf.* in 2003 and 2007. An approximate 111 km<sup>2</sup> extension was found, delimited to the west by the Skaftafellsá river and to the east by the estuary of the Fjallsá river.

Information given by Thorarinsson (1958) and Roberts and Gudmundsson (2015) was used to estimate the threat posed by debris and water temperature.

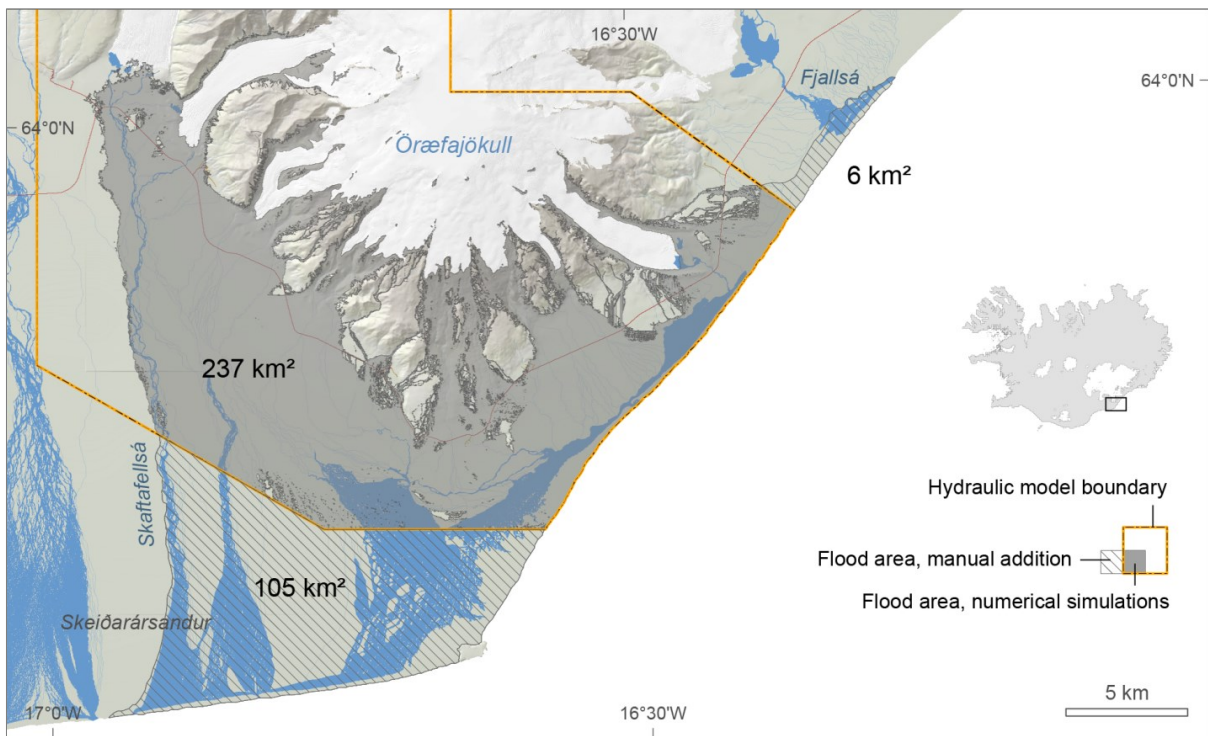


Figure V-7: Areas identified at risk of flooding in Helgadóttir *et al.* (2015). The flood area identified in the numerical simulations is shown in grey; extension of the flood area beyond the boundaries of the hydraulic model does show as a striped pattern.

## 5. Results

### 5.1. Markarfljót outwash plain

Flood-hazard rating was performed using the depths of flooding  $d$  only. Flow velocities, water temperature and debris load were not investigated thoroughly for this area and therefore not used in the rating.

Flood hazard was rated as *high* (depths ranging 1–6 m) or *extreme* (depths in excess of 6 m) on 384 and 332 km<sup>2</sup> of land, respectively, representing together 85% of the design flood area (Table V-6, Figure V-8). The extreme hazard zone is limited to the west by road 255 (Akureyjarvegur). Areas where flood hazards were rated as *low* ( $d < 0.5$  m) or *moderate* ( $d$  ranging 0.5–1 m) only

represent ~10% of the flood area and are mainly located between the Rangá and Þjórsá rivers. Although depths of flooding in the manual addition to the flood area, south from Eyjafjallajökull volcano, could have been

inferred to a certain degree from contiguous depth values, flood hazard in the above-mentioned area was provisionally set to *undetermined*.

Table V-6: Provisional rating of flood hazard in the Markarfljót outwash plain, using depths of flooding computed by Hólm and Kjaran (2005). The extreme hazard area (i.e. area of total devastation) represents ~40% of the flood area.

Hazard rate	Flood area, numerical simulation		Flood area, manual addition		Total	
	km <sup>2</sup>	%	km <sup>2</sup>	%	km <sup>2</sup>	%
Undetermined	0	0	33	100	33	4
Low	61	8	0	0	61	7
Moderate	33	4	0	0	33	4
High	384	47	0	0	384	46
Extreme	332	41	0	0	332	39
<b>Total</b>	<b>810</b>	<b>100</b>	<b>110</b>	<b>100</b>	<b>346</b>	<b>100</b>

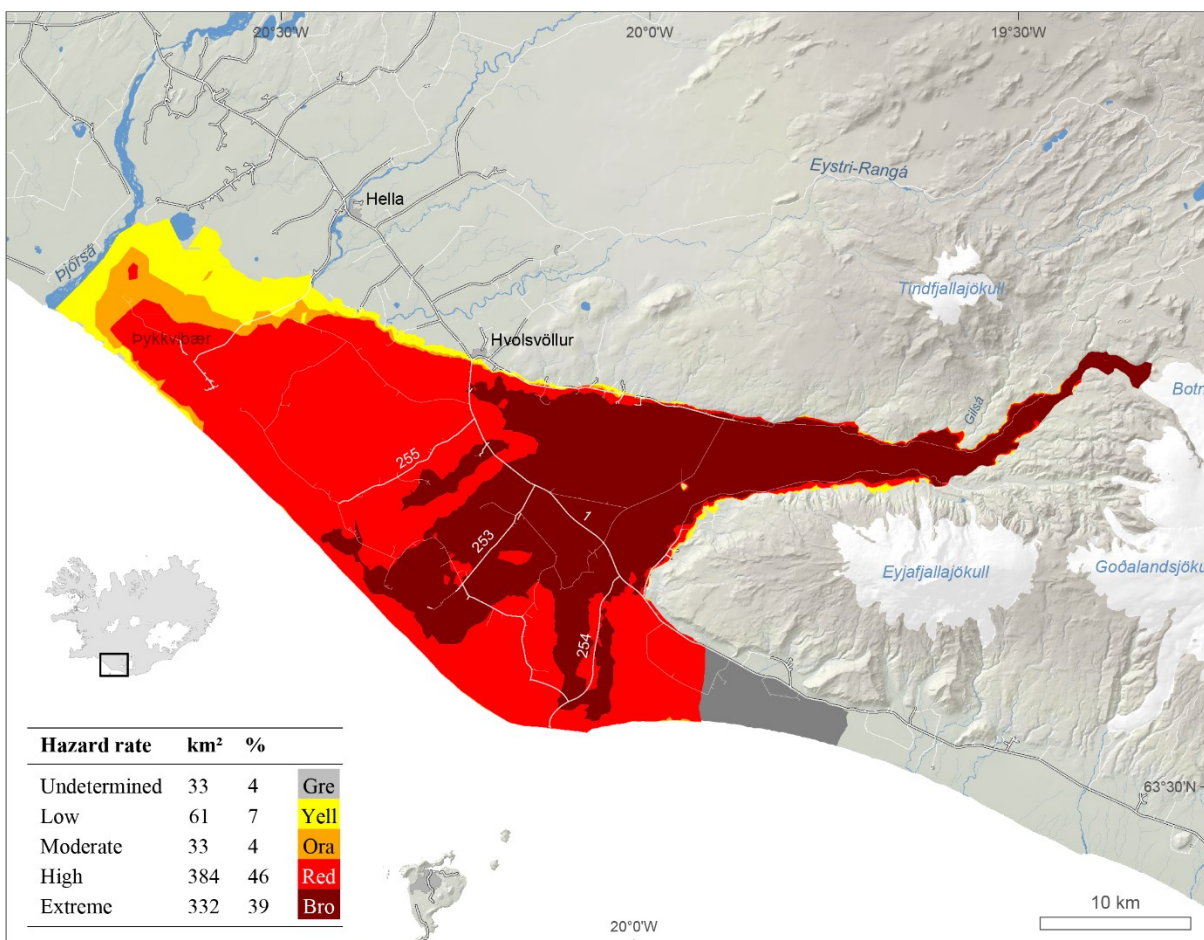


Figure V-8: Provisional rating of flood hazard in the Markarfljót outwash plain, using depths of flooding computed by Hólm and Kjaran (2005).

## 5.2. Öraefi district

Rating of flood hazard was performed using depth-velocity products  $dv$ , debris load  $l$ , and water temperature  $t$ .

### 5.2.1. Depth-velocity product

Based on depth-velocity products  $dv$ , flood hazard was rated as *high* or *extreme* on respectively ~12% (29 km<sup>2</sup>) and ~77% (183 km<sup>2</sup>) of the flood area identified in the numerical simulations (Table V-7). Only 10% of the computed flood area was rated as *low* or *moderate* hazard areas

### 5.2.2. Debris and sediments

Geomorphic evidence of past flooding events indicates that the area identified at risk of flooding in the simulations performed by Helgadóttir *et al.* (2015) is certainly exposed to flows of debris including clasts of glacier ice and boulders exceeding hundreds of tonnes. During the 1362 jökulhlaup, angular-shaped boulders weighing > 500 tons were transported by floodwaters from the Fall-

jökull glacier and left interbedded with sediments, ~4 km from the glacier margin (Roberts and Gudmundsson, 2015 and references therein). It has also been reported that during the 1727 jökulhlaup many icebergs were transported to the sea (Thorarinsson, 1958). The thickness of sediments transported by floodwaters was also important enough to bury completely structures and people. At the base of Öraefajökull, modern-day exposures of sediments deposited during the 1727 jökulhlaup range from metres to tens of metres in depth. At distances exceeding 7 km from the edge of the ice cap, metre-scale sections of jökulhlaup sediments are apparent, signifying that large volumes of eruptive material and pre-existing sandur deposits were mobilised by volcanogenic floods. Throughout the same region, grain sizes range from coarse sands to boulders in excess of 5 m in diameter.

The debris index  $l$  was therefore set to 1 at every location of the computed flood area and of the manual addition.

Table V-7: Hazard rating of the flood area identified in the numerical simulations by Helgadóttir *et al.* (2015), using depth-velocity products.

Hazard rate	code	km <sup>2</sup>	%
Low	1	4	1.7
Moderate	2	20	8.5
High	3	29	12.4
Extreme	4	183	77.4

### 5.2.3. Water temperature

Highly variable water temperatures can be expected at the vicinity of the glaciers should an eruption happen. It has been reported for instance that the temperature of torrents, a few kilometres from the Kotárjökull glacier margin, was warm enough days after the 1727 jökulhlaup to prevent horses from wading in waters (Thorarinsson, 1958).

At the onset of the eruption, while floodwater is in sustained contact with glacial ice, near-freezing water temperatures can be expected.

As a result, the floodwater temperature index  $t$  was set to 1 at every location of the computed flood area and of the manual addition.

### 5.2.4. Computed hazard rate

Flood hazard was finally rated as *high* or *extreme* on 164 km<sup>2</sup> (47%) and 183 km<sup>2</sup> (53%) of land, respectively (Figure V-9,

Table V-8). The share of *extreme* hazard is certainly higher in reality, as the depth-velocity products could not be computed beyond the boundaries of the hydraulic model.

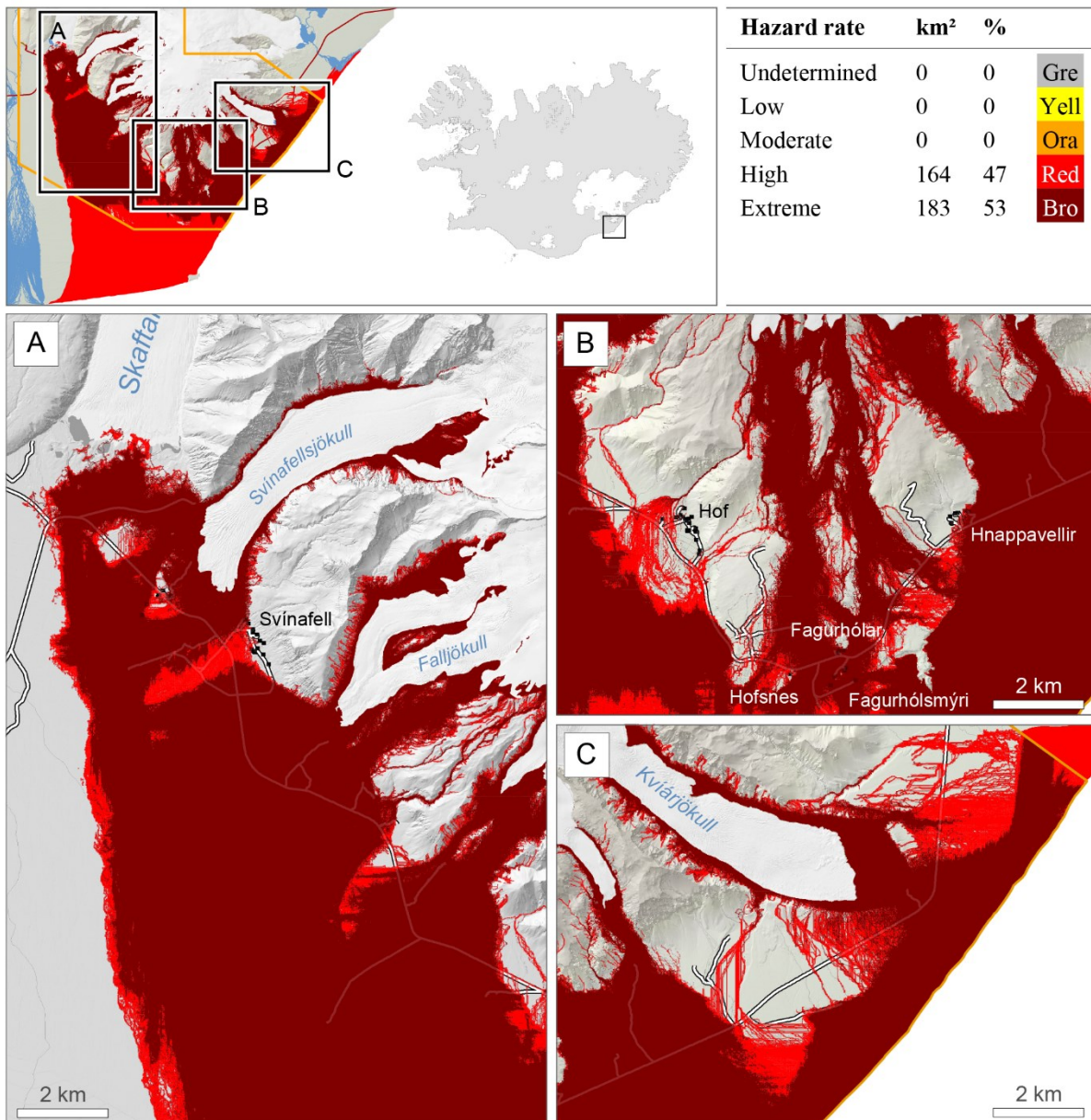


Figure V-9: Provisional rating of flood hazards due to eruptions of Örfajökull volcano. Depths of flooding and flow velocities computed by Helgadóttir et al. (2015) were used, along with considerations on debris and water temperature. The extreme hazard area (i.e. area of total devastation) represents ~53% of the flood area.

Table V-8: Provisional rating of flood hazards due to eruptions of Öraefajökull; depths of flooding and flow velocities computed by Helgadóttir et al. (2015) were used, along with considerations on debris and water temperature. The extreme hazard area represents 53% of the flood area.

Hazard rate	Flood area, numerical simulations		Flood area, manual addition		Total	
	km <sup>2</sup>	%	km <sup>2</sup>	%	km <sup>2</sup>	%
Undetermined	0	0	0	0	0	0
Low	0	0	0	0	0	0
Moderate	0	0	0	0	0	0
High	54	23	110	100	164	47
Extreme	183	77	0	0	183	53
Total	237	100	110	100	347	100

## 6. Discussion

### 6.1. Methodological limits

Several aspects should be considered carefully when rating of flood hazard is performed, or when use is made of flood hazard rates, using the methodology proposed.

#### 6.1.1. Input parameters

Using alternatively depths of flooding (hydrostatic forces), velocities or dynamic pressures, and depth-velocity products does not give similar results. Using either depth of

flooding or dynamic pressure alone leads to a significant downgrading of hazard rates obtained with the depth-velocity product. In the Öraefi district, the area where flood hazard is rated as extreme using depths of flooding only covers 116 km<sup>2</sup> of land, which is ~40% less than by using the  $dv$  product (Table V-9).

As the depth-velocity product takes into account both hydrostatic and hydrodynamic forces, it is assumed to reflect real conditions better than either depths of flooding or dynamic pressure, and therefore should receive precedence in the rating of flood hazard when available.

Table V-9: Spatial extent of extreme hazard areas, based on either depths of flooding or depth-velocity products.

	depths of flooding $d$	depth-velocity product $dv$
Lower threshold	6 m	7 m <sup>2</sup> /s
Spatial extent (km <sup>2</sup> )	116	183
Spatial extent (%)*	49	77
Spatial extent (%)**	63	100

\* As share of the total flood area identified in numerical simulations

\*\* As share of the area where flood hazard is rated as extreme according to the depth-velocity product

### 6.1.2. Switching between rates

Switching from *moderate* hazard to *high* hazard represents a qualitative jump in terms of injuries and fatalities: danger is for all where hazard is rated *high* while it is for some (disabled, elderly, and children) where hazard is rated *moderate*. The extreme hazard class is primarily aimed at identifying areas where 100% destruction is expected (during events or afterwards, in the recovery phase). Such information should be useful when an effort is made on quantifying monetary losses due to direct damages inflicted to physical assets (e.g. van Vesten *et al.*, 2014).

## 6.2. Reproducibility

The presence of life-threatening debris and temperature of floodwater were considered, along with depths of flooding and flow velocities, in a flood hazard rating methodology that account for the unique nature of jökulhlaups. The methodology was devised to be used for the delineation of flood hazard zones in Icelandic areas prone to volcanogenic floods, provided that enough information on flood hazard characteristics therein can be acquired and processed. Use of the methodology is not bound to be used in the Markarfljót outwash plain and the Öraefi district only.

As the flood hazard characteristics considered, and the thresholds retained, are also valid for tsunamis (e.g. Leone *et al.*, 2010; Valencia *et al.*, 2011) and riverine floods, including ice-jam floods (e.g. Pagneux and Snorrason, 2012) and flooding due to dam break (e.g. Karvonen *et al.*, 2000), an application of the methodology to types of floods other than jökulhlaups can also be envisaged.

## 7. Summary and conclusion

A semi-quantitative rating of flood hazards focusing on flood damage potential was proposed and flood hazard zones designated accordingly in the Markarfljót outwash plain and in the Öraefi district, two Icelandic

regions that have experienced jökulhlaups due to subglacial eruptions in the last 1000 years.

Using alternatively depths of flooding or the product of flow velocities and flood depths on one hand, the presence of life-threatening debris and temperature of floodwater on the other (Table V-4), a distinction was made between four hazard rates:

- **Low hazard**

Injuries or fatalities are unlikely; damages are mostly limited to furniture inside buildings.

- **Moderate hazard**

Danger is for some, including children, the elderly and the infirm, inside and outside buildings. Damage to buildings is expected but the structural integrity of buildings remains preserved.

- **High hazard**

All lives are in jeopardy, outside and inside inhabited buildings. The risk of drowning is significant as the wading limit for a normalised adult is reached; severe injuries or fatalities due to debris load and floodwater temperature are expected. Partial or total collapse of light buildings is expected due to scouring, buoyancy, and lateral pressures exerted against walls.

- **Extreme hazard**

Total destruction of non-reinforced buildings is expected; structural damages to reinforced concrete dwellings are expected to a degree that does require demolition in the recovery phase.

An application of the method to the two study areas indicates a potential for significant direct economic damage and fatalities:

- **Markarfljót outwash plain**

Based on maximum depths of flooding, flood hazard was rated as *high* or *extreme* on respectively 384 and 332 km<sup>2</sup> of land, i.e. 85% of the flood area (Figure V-8). Extent of the high-hazard area may increase upon

integration of flow velocities, water temperature, and debris load.

### • Öraefi district

Using the depth-velocity product as well as information on water temperature index and debris load, flood hazard was exclusively rated as *high* or *extreme* on 164 km<sup>2</sup> and 183 km<sup>2</sup> of land, respectively (Figure V-9).

As a first approximation of damage potential due to volcanogenic floods in the two areas, these results should be carefully considered by the local and national authorities when evacuation procedures and planning on the long term are discussed. The spatial boundary between hazard rates depends much on which and how flood characteristics are used. It should be noted, in particular, that using depths of flooding alone leads to a significant downgrading of hazard rates obtained with the depth-velocity product. As the depth-velocity product accounts for both hydrostatic and hydrodynamic forces, it is assumed to reflect real conditions better than depths of flooding alone and therefore should receive precedence in the rating of flood hazard when available.

## 8. Acknowledgements

The authors would like to thank Frédéric Leone, Tómas Jóhannesson, and Trausti Jónsson for their review and proof-reading of the chapter. Oddur Sigurðsson is thanked for provision of photographs.

The present work was funded by the Icelandic Avalanche and Landslide Fund, the National Power Company, and the Icelandic Road and Coastal Administration.

## 9. References

- Abt, S. R., Whittker, R. J., Taylor, A., & Love, D. J. (1989). Human stability in a high flood hazard zone. *Water Res. Bull.*, 25, 881–890.
- Akbas, S. O., Blahut, J., & Sterlacchini, S. (2009). Critical assessment of existing physical vulnerability estimation approaches for debris flows. In J. P. Malet, A. Remaître, & T. A. Bogaard (Ed.), *International Conference*
- "Landslide Processes" (pp. 229–233). Strasbourg: CERG Editions.
- Barbolini, M., Cappabianca, F., & Sailer, R. (2004). Empirical estimate of vulnerability relations for use in snow avalanche risk assessment. In C. Brebbia (Ed.), *Risk analysis IV* (pp. 533–542). Southampton: WIT Press.
- Black, R. (1975). *Flood Proofing Rural Residences*. New York: Department of Agricultural Engineering, Cornell University.
- Clausen, L., & Clark, P. (1990). The development of criteria for predicting dambreak flood damages using modelling of historical dam failures. In W. R. White (Ed.), *International Conference on River Flood Hydraulics* (pp. 369–380). John Wiley & Sons Ltd.
- de Moel, H., van Alphen, J., & Aerts, J. (2009). Flood maps in Europe - Methods, availability and use. *Nat. Hazards Earth Syst. Sci.*, 9, 289–301.
- DEFRA (2006). *Flood risk to people. Phase 2*. London: Environment Agency and Department for Environment, Food and Rural Affairs.
- DEFRA (2008). *Supplementary note on flood hazard ratings and thresholds for development planning and control purpose. Clarification of the Table 13.1 of FD230/TR2 and figure 3.2. of FD2321/TR1*. London: Environment Agency and Department for Environment, Food and Rural Affairs.
- Dutta, D., Herath, S., & Musiaka, K. (2003). A mathematical model for flood loss estimation. *Journal of Hydrology*, 277, 24–49.
- Environment Canada. (1993). *Flooding: Canada Water Book* (Andrews, J. ed.). Ottawa: Economics and Conservation Branch, Ecosystem Sciences and Evaluation Directorate, Environment Canada.
- EXCIMAP (2007). *Handbook on Good Practices for Flood Mapping in Europe*. (F. Martini, & R. Loat, Eds.) The Hague: Netherland Ministry of Transport, Public Works and Water Management.
- Foster, D. N., & Cox, R. J. (1973). *Stability of children on roads used as floodways*. Manly vale, New South Wales, Australia: Water Research Laboratory, The University of New South Wales.
- Fraser, S., Raby, A., Pomonis, A., Goda, K., Chian, S. C., Macabuag, J., Offord, M., Saito, K., and Sammonds, P. (2013). Tsunami damage to coastal defences and buildings in the March 11th 2011 Mw 9.0 Great East Japan earthquake and tsunami. *Bull. Earthquake Eng.*, 11, 205–239.

- French, J., Ing, R., von Allmen, S., & Wood, R. (1983). Mortality from flash floods: A review of National Weather Service Reports, 1969-1981. *Public Health Reports*, 98(6), 584–588.
- Fuchs, S., Heiss, K., & Hübl, J. (2007). Towards an empirical vulnerability function for use in debris flow risk assessment. *Nat. Hazards Earth Syst. Sci.*, 7, 495–506.
- Gudmundsson, M. T., Högnadóttir, Þ., & Magnússon, E. (2015). Öraefajökull: Eruption melting scenarios. In E. Pagneux, M. T. Gudmundsson, S. Karlsdóttir, & M. J. Roberts (Eds.), *Volcanogenic floods in Iceland: An assessment of hazards and risks at Öraefajökull and on the Markarfljót outwash plain* (pp. 45–72). Reykjavík: IMO, IES-UI, NCIP-DCPEM.
- Gudmundsson, M. T., Larsen, G., Höskuldsson, Á., & Gylfason, Á. G. (2008). Volcanic hazards in Iceland. *Jökull*, 58, 251–258.
- Guðmundsson, M. T., Elíasson, J., Larsen, G., Gylfason, Á. G., Einarsson, P., Jóhannesson, T., Hákonardóttir, K. M., and Torfason, H. (2005). Yfirlit um hættu vegna eldgosa og hlaupa frá vesturhluta Mýrdalsjökuls og Eyjafjallajökli (Overview of hazards due to volcanic eruptions and volcanogenic floods on the western slopes of Mýrdalsjökull and Eyjafjallajökull). In M. T. Guðmundsson, & Á. G. Gylfason (Eds.), *Hættumat vegna eldgosa og hlaupa frá vestanverðum Mýrdalsjökli og Eyjafjallajökli (Hazard assessment of volcanic eruptions and glacial outbursts for Eyja-fjallajökull and the western outwash plain of Mýrdalsjökull)* (pp. 11–44). Reykjavík: National Commissioner of Police.
- Helgadóttir, Á., Pagneux, E., Roberts, M. J., Jensen, E. H., & Gíslason, E. (2015). Öraefajökull Volcano: Numerical simulations of eruption-induced jökulhlaups using the SAMOS flow model. In E. Pagneux, M. T. Gudmundsson, S. Karlsdóttir, & M. J. Roberts (Eds.), *Volcanogenic floods in Iceland: An assessment of hazards and risks at Öraefajökull and on the Markarfljót outwash plain* (pp. 73–100). Reykjavík: IMO, IES-UI, NCIP-DCPEM.
- Hólm, S. L., & Kjaran, S. P. (2005). Reiknilíkan fyrir útbreiðslu hlaupa úr Entujökli (Hydraulic model of floods from Entujökull). In M. T. Guðmundsson, & Á. G. Gylfason (Eds.), *Hættumat vegna eldgosa og hlaupa frá vestanverðum Mýrdalsjökli og Eyjafjallajökli (Hazard assessment of volcanic eruptions and glacial outbursts for Eyjafjallajökull and the western outwash plain of Mýrdalsjökull)* (pp. 197–210). Reykjavík: National Commissioner of Police.
- Jonkman, S. N., & Kelman, I. (2005). An analysis of the causes and circumstances of flood deaths. *Disasters*, 29(1), 75–95.
- Jonkman, S. N., & Penning-Rowsell, E. (2008). Human instability in flood flows. *Journal of the American Water Resources Association*, 44(4), 1–11.
- Jóhannesson, T., Björnsson, H., Magnússon, E., Guðmundsson, S., Pálsson, F., Sigurðsson, O., Thorsteinsson, T., and Berthier, E. (2013). Ice-volume changes, bias estimation of mass-balance measurements and changes in subglacial lakes derived by lidar mapping of the surface of Icelandic glaciers. *Annals of Glaciology*, 54(63), 63–74.
- Jóhannesson, T., Björnsson, H., Pálsson, F., Sigurðsson, O., & Thorsteinsson, T. (2011). LiDAR mapping of the Snæfellsjökull ice cap, western Iceland. *Jökull*, 61, 19–32.
- Karvonen, R. A., Hepojoki, A., Huhta, H., & Louhio, A. (2000). *The use of physical models in dam-break analysis. RESCDAM Final Report*. Helsinki: Helsinki University of Technology.
- Keller, R. J., & Mitsch, B. (1993). *Safety aspects of the design of roadways as floodways. Final report for Urban Water Research Association, Melbourne Water Research Project*. Melbourne: Monash University.
- Kelman, I., & Spence, R. (2004). An overview of flood actions on buildings. *Engineering Geology*, 73, 297–309.
- Kemmerling, G. L. (1921). De uitbarsting van den G. Keloet in den nacht van den 19den op den 20sten mei 1919 (The eruption of Mount Kelud on the May 19–20 1919 night). *Vulkanol Mededeel*, 2.
- Kreibich, H., & Dimitrova, B. (2010). Assessment of damages caused by different flood types. In D. Wrachien, D. Proverbs, C. A. Brebbia, & S. Mambretti (Eds.), *Flood Recovery, Innovation and Response II* (Vol. 133, pp. 3–11). Southampton: WIT Press.
- Kreibich, H., Piroth, K., Seifert, I., Maiwald, H., Kunnert, U., Schwarz, J., Merz, B., and Thieken, A. H. (2009). Is flow velocity a significant parameter in flood damage modelling? *Nat. Hazards Earth Syst. Sci.*, 9, 1679–1692.
- Leone, F., Lavigne, F., Paris, R., Denain, J. C., & Vinet, F. (2010). A spatial analysis of the December 26th, 2004 tsunami-induced damages: Lessons learned for a better risk assessment integrating buildings vulnerability. *Applied Geography*, 31(1), 363–375.
- Lloyd, E. L. (1996). Accidental hypothermia. *Resuscitation*, 32(2), 111–24.

- Luna, B. Q., Blahut, J., van Westen, C. J., Sterlacchini, S., van Asch, T. W., & Akbas, S. O. (2011). The application of numerical debris flow modelling for the generation of physical vulnerability curves. *Nat. Hazards Earth Syst. Sci.*, *11*, 2047–2060.
- MATE/METL (2002). *Plans de Prévention des Risques Naturels (PPR): Risques d'inondation. Guide méthodologique (Prevention Plans against Natural Hazard Risks: Flooding Risks. Methodological guide)*. Paris: La Documentation Française.
- Merz, B., Kreibich, H., Schwarze, R., & Thieken, A. H. (2010). Assessment of economic damage. *Nat. Hazards Syst. Sci.*, *10*, 1697–1724.
- Mileti, D., Bolton, P., Fernandez, G., & Updike, R. (1991). *The eruption of Nevado del Ruiz Volcano Colombia, South America, November 13, 1985*. (Commission on Engineering and Technical Systems, Ed.) Washington D.C.: National Academy Press.
- Ministry for the Environment. (2000). Reglugerð 505/2000 um hættumat vegna ofanflóða, flokkun og nýtingu hættusvæða og gerð bráða-birgðahættumats (Regulation 505/2000 on the risk assessment of avalanches and shallow slides, classification and use of risk zones, and making of...). Reykjavík: Government Offices of Iceland.
- Ministry for the Environment and Natural Resources. (2013). Skipulagsreglugerð 90/2013. Reykjavík: Government Offices of Iceland.
- NARA (2009). Flood plain management and protection of wetlands. In *U.S. Code of Federal Regulations, Title 44, Vol. 1, Chapter 1, part 9* (pp 69–88).
- Pagneux, E. (2015a). Öraefi district and Markarfljót outwash plain: Spatio-temporal patterns in population exposure to volcanogenic floods. In E. Pagneux, M. T. Gudmundsson, S. Karlsdóttir, & M. J. Roberts (Eds.), *Volcanogenic floods in Iceland: An assessment of hazards and risks at Öraefajökull and on the Markarfljót outwash plain* (pp. 123–140). Reykjavík: IMO, IES-UI, NCIP-DCPEM.
- Pagneux, E. (2015b). Öraefajökull: Evacuation time modelling of areas prone to volcanogenic floods. In E. Pagneux, M. T. Gudmundsson, S. Karlsdóttir, & M. J. Roberts (Eds.), *Volcanogenic floods in Iceland: An assessment of hazards and risks at Öraefajökull and on the Markarfljót outwash plain* (pp. 141–164). Reykjavík: IMO, IES-UI, NCIP-DCPEM.
- Pagneux, E., & Snorrason, Á. (2012). High-accuracy mapping of inundations induced by ice-jams: a case-study from Iceland. *Hydrology Research*, *43*(4), 412–421.
- Parliament of Iceland. (2010). Skipulagslög 123/2010 (Planning Act 123/2010).
- Penning-Rowsell, E., Johnson, C., Tunstall, S., Tapsell, S., Morris, J., Chatterton, J., & Green, C. (2005). *The Benefits of Flood and Coastal Risk Management: A Handbook of Assessment Techniques*. London: Middlesex University Press.
- Reiter, P. (2000). Considerations on urban areas and floating debris in dam-break flood modelling. *RESCDAM seminar, Session 2, Mathematical and physical modelling to simulate a dam-break flood*.
- Roberts, M. J., & Gudmundsson, M. T. (2015). Öraefajökull Volcano: Geology and historical floods. In E. Pagneux, M. T. Gudmundsson, S. Karlsdóttir, & M. J. Roberts (Eds.), *Volcanogenic floods in Iceland: An assessment of hazards and risks at Öraefajökull and on the Markarfljót outwash plain* (pp. 17–44). Reykjavík: IMO, IES-UI, NCIP-DCPEM.
- Roberts, M. J., Sigurðsson, G., Sigurðsson, O., Pagneux, E., Jóhannesson, T., Zóphóníasson, S., Gudmundsson, M. T., Russell, A. J., Gylfason, Á. G., Höskuldsson, F., and Björnsson, B. B. (2011). The April 2010 Eruption of Eyjafjallajökull Volcano: Glacial flooding and attendant hazards. *IAVCEI Symposium Surface processes in volcanic terrains: the erosion, transport and redeposition of volcanoclastic material and their associated hazards*. Melbourne.
- Russell, A. J., Tweed, F., Roberts, M. J., Harris, T. D., Gudmundsson, M. T., Knudsen, O., & Marren, P. M. (2010). An unusual jökulhlaup resulting from subglacial volcanism, Sólheimajökull, Iceland. *Quaternary Science Review*, 1363–1381.
- Russo, B., Gómez, M., & Macchione, F. (2013). Pedestrian hazard criteria for flooded urban areas. *Nat. Hazards*, *69*, 251–265.
- Schwarz, J., & Maiwald, H. (2008). Damage and loss prediction model based on the vulnerability of building types. *4th International Symposium on Flood Defence: Managing Flood Risk, Reliability and Vulnerability*. Toronto.
- Smith, D. I. (1991). Extreme floods and dam failure inundation implications for loss assessment. *Proceedings of a Seminar "Natural and Technological Hazards: Implications for the Insurance Industry"*, (pp. 149–165).
- Snorrason, Á., Einarsson, B., Pagneux, E., Hardardóttir, J., Roberts, M., Sigurðsson, O., Thórarinsson, Ó., Crochet, P., Jóhannesson, T., and Thorsteinsson, T. (2012). Floods in Iceland. In Z. W. Kundzewicz (Ed.), *Changes in flood risk in Europe* (pp. 257–276). IAHS Special Publication 10.

- Thorarinnsson, S. (1958). The Öräfajökull eruption of 1362. *Acta Naturalia Islandica*, 2(4), 100.
- Tinti, S., Tonini, R., Bressan, L., Armigliato, A., Gardi, A., Guillaude, R., Valencia, N., and Scheer, S. (2011). *Handbook of tsunami hazard and damage scenarios*. Luxembourg: Publications Office of the European Union.
- USBR (U.S. Department of the Interior, Bureau of Reclamation). (1988). *Downstream Hazard Classification Guidelines*. Denver: USBR.
- Valencia, N., Gardi, A., Gauraz, A., Leone, F., & Guillaude, R. (2011). New tsunami damage functions developed in the framework of SCHEMA project: application to European-Mediterranean coasts. *Nat. Hazards Earth Syst. Sci.*, 11, 2835–2846.
- Van Vesten, C., Kappes, M. S., Luna, B. Q., Frigerio, S., Glade, T., & Malet, J. P. (2014). Medium-scale multi-hazard risk assessment of gravitational processes. In T. Van Asch, J. Corominas, S. Greiving, J. P. Malet, & S. Sterlacchini (Eds.), *Mountain risks: From prediction to management and governance*. London: Springer.
- Voigt, B. (1990). The 1985 Nevado del Ruiz volcano catastrophe: anatomy and restrospection. *Journal of Volcanology and Geothermal Research*, 44, 349–386.
- Wilhelm, C. (1998). Quantitative risk analysis for evaluation of avalanche protection projects. *Proceedings of the 25 Years of Snow Avalanche Research* (pp. 288–293). Oslo: NGI Publications.